Differential Adhesion of Microspheres Mediated by DNA Hybridization I: Experiment

Ying Zhang,*† Valeria T. Milam,*† David J. Graves,*‡ and Daniel A. Hammer*†‡
Departments of *Chemical and Biomolecular Engineering and ‡Bioengineering, and †Institute for Medicine and Engineering, University of Pennsylvania, Philadelphia, Pennsylvania 19104

ABSTRACT We have developed a novel method to study collective behavior of multiple hybridized DNA chains by measuring the adhesion of DNA-coated micron-scale beads under hydrodynamic flow. Beads coated with single-stranded DNA probes are linked to surfaces coated with single target strands through DNA hybridization, and hydrodynamic shear forces are used to discriminate between strongly and weakly bound beads. The adhesiveness of microspheres depends on the strength of interaction between DNA chains on the bead and substrate surfaces, which is a function of the degree of DNA chain overlap, the fidelity of the match between hybridizing pairs, and other factors that affect the hybridization energy, such as the salt concentration in the hybridization buffer. The force for bead detachment is linearly proportional to the degree of chain overlap. There is a detectable drop in adhesion strength when there is a single base mismatch in one of the hybridizing chains. The effect of single nucleotide mismatch was tested with two different strand chemistries, with mutations placed at several different locations. All mutations were detectable, but there was no comprehensive rule relating the drop in adhesive strength to the location of the defect. Since adhesiveness can be coupled to the strength of overlap, the method holds promise to be a novel methodology for oligonucleotide detection.

INTRODUCTION

DNA is the fundamental genetic material in organisms and is often found in the format of double helix. The force that holds complementary strands of DNA together is an important regulator of life's processes, because the binding of regulatory proteins to DNA often involves the procedure of mechanical separation of its strands. Therefore, the intermolecular forces of DNA have been studied extensively. Most work on the force to disengage short duplexes was performed with atomic force microscope (1–4). Lee et al. measured the unbinding force between two DNA molecules with repeating sequences (1). Strunz and co-workers (4) studied the force to dissociate the DNA sequences with different overlap lengths, and they found that the force and time for the dissociation of bound DNA chains followed the Bell model (5,6),

$$k_r = k_r^o \exp(\gamma F/k_b T),$$

where k_r is the dissociation rate, k_r^0 is the unstressed dissociation rate constant, γ is the reactive compliance, F is the applied force, k_b is the Boltzmann constant, and T is the temperature. Both k_r^0 and γ were functions of the degree of chain overlap, N, and they decrease with increasing N. Force between strands of DNA with defective base-matching were studied by Sattin et al., and the forces between strands of DNA were derived (7).

Although extensive work has been done on a single hybridized pair, very few results have been reported about the collective behavior of multiple hybridized chains in an adhesive interface (8). The cumulative result of dissociation force is particularly interesting because thermodynamic fluctuations can be ignored if a large number of molecules mediate adhesion simultaneously. Moreover, multiple chain interactions have been shown to result in sharpened dependence on variables that influence adhesion, such as temperature in the case of nanospheres (9,10). If dissociation force is used as a selection pressure to discriminate between chains of different overlap, the interaction between multiple chain pairs can be expected to provide a method with better sensitivity through a collective behavior that sharpens the relationship between chemistry and force.

In this article, we describe a microsphere adhesion system mediated by DNA hybridization. We gain insight into DNA-mediated adhesive behavior through previous work on the receptor-mediated adhesion of beads (11–13). The adhesion of beads under flow is a result of the balance between receptor-mediated forces and hydrodynamic force applied on the bead by controlled flow. The net adhesiveness of the particle is the result of the number of specific, macromolecular bonds between the bead and the surface and their strength, which are related to the properties of the individual receptors. The fundamental interactions of leukocyte adhesion receptors have been studied by controlling the hydrodynamic force applied on the receptor-coated beads (14–17). Also, the affinity between antibody and antigen could be deduced from detachment experiments of antibody-coated beads bound to surfaces (12,13). By analogy, because of the high affinity and high specificity of DNA interactions, we would expect that microsphere adhesion can be used to measure the DNA-mediated adhesion strength and that, with the proper analysis, the adhesion force can be used to deduce properties of hybridized single chains during detachment.

Submitted August 12, 2005, and accepted for publication December 27, 2005.

Address reprint requests to Daniel A. Hammer, Dept. of Bioengineering, University of Pennsylvania, 120 Hayden Hall, 3320 Smith Walk, Philadelphia, PA 19104. Tel.: 215-573-6761; Fax: 215-573-2071; Email: hammer@seas.upenn.edu.

0006-3495/06/06/4128/09 $2.00

doi: 10.1529/biophysj.105.072629

Conversely, we hypothesized that using hydrodynamic forces would allow us to discriminate between weakly and strongly bound adhesive pairs, thus providing a means of coupling the fidelity of DNA binding to adhesion strength. In turn, adhesion strength could then be used as a metric of DNA binding strength.

Besides elucidating the fundamental physics of DNA-DNA binding, another goal of our work is to develop a novel system for detection of specific DNA hybridization on microarray surface. As an alternative to Southern or Northern blotting experiments, DNA microarray technology is considered a revolution in molecular biology and medicine (18–21). This technology is used to measure the concentration of messenger RNA in living cells, detect mutations in specific genes, or identify unknown genes from foreign cells (18). In a typical DNA microarray, single-stranded oligonucleotides are immobilized on a glass, silicon, or plastic substrate surface, and then allowed to contact and hybridize with complementary molecules in the solution (22). Hybridization analysis involves detecting the signal generated by the binding of fluorescently labeled probe DNA or RNA sequences, and comparing the fluorescent intensities with those of the reference sample (23). Hybridization efficiency determined from this comparison is correlated to the concentration of specific nucleotides in sample and their chemistry. Though powerful, there are limitations in this technology, some of which include dye photobleaching, low signal/noise ratios, and the difficulty of determining statistically and biologically meaningful positive matches (9,24). Therefore, alternative methods have been developed to improve traditional microarray techniques (9,24–27). Cao et al. used gold nanoparticles linked to oligonucleotides that can act as Raman-active dyes. Probe strands are linked to these particles, which are then hybridized to the target sequences on the chip. After silver enhancement, this system was able to detect probe strands at a concentration of 100 aM (27). Miller et al. described a multianalyte biosensor that used magnetic microbeads as the label to detect DNA hybridization on a microfabricated chip (28). After binding to immobilized DNA, probes containing a mass-labeled moiety in Schatz et al.'s work released the mass to allow the hybridization to be characterized by MALDI mass spectroscopy (29). Other detection methods are also being investigated. Differences in specific boundary conditions at a liquid-solid interface, such as charge density, mass, viscosity, and molecular structure before and after probe binding have been measured to characterize the hybridization (30–33). Exploiting the association and dissociation kinetics of nucleic acid binding, surface plasmon resonance and surface plasmon fluorescence spectroscopy were observed to have an efficient discriminatory power with respect to single-base mismatch hybridization (32–34).

Our work described in this article develops a fluorochrome-free detection system generating optical signals with particles in low micrometer size range. Serving as visible tags, such large particles potentially can provide advantages of still greater amplification of the signal, as well as a relatively simple instrument for resulting readouts, and even the possibility of producing an instrument-free (naked eye) detection system. Since hydrodynamic shear forces scale with the square of particle radius, it is possible to use hydrodynamic shear forces as a selection pressure to discriminate between well and weakly bound pairs; this would not be possible with nanospheres. In addition, such large spheres can interact with bound chains through a large number of chain-chain interactions, creating an adhesion ''patch'' between each bead surface and substrate surface. As mentioned previously, the cooperative effects of multiple immobilized strands between surfaces result in sharpened dependence on variables influencing specific adhesion. Consequently, at large enough flow rates (35), we hypothesize that the adhesion ''patch'' containing multiple hybridized chains will increase sensitivity to hydrodynamic force, under which imperfectly matched hybridizing chains will separate. Moreover, the bond density within this ''patch'' can be increased effectively by increasing the concentration of molecules on a particle surface, without increasing the total number of DNA molecules in the hybridization buffer. Therefore, the combination of cooperativity and hydrodynamic forces may provide a better method of distinguishing perfectly complementary nucleotide chains from those where there is a single-base mismatch (23).

In this article, we report on experiments in which microspheres coated with single-stranded probe oligonucleotides are allowed to contact a surface covered with single-stranded target oligonucleotides in the absence of hydrodynamic flow, and then the particles are detached from the surface by applying a constant shear stress. Oligonucleotide molecules are immobilized on microspheres via biotin-avidin bonds, and linked to a glass slide covalently. After a gentle wash to remove nonadherent beads, only microspheres functionalized with complementary base matching immobilized probe strands remain on the substrate. We then relate the relative adhesive strength between DNA chains by applying shear stress to find the critical shear rate necessary to remove 50% of the beads. Critical shear rates for particle detachment are correlated with the degree of chain overlap and other factors that affect the energy of probe-target hybridization, such as the salt concentration in the hybridization buffer. Furthermore, we explore the adhesion strength resulting from the presence of single point mutation in DNA pairs and compare it with the strength mediated by perfectly hybridized chains, and examine how the location of the mutation affects adhesion strength. The results show that micron-sized colloidal particles can be engineered to adhere specifically to a surface, and adhesion strength can be effectively used to discriminate between probe-target pairs of different overlap length, as well as to determine the effect of point mutations. Overall, this article describes an effective method to study the biophysics of multiple hybridized DNA molecules and

develops a promising method, combining adhesion under hydrodynamic flow, readily detectable micron-sized colloids, and DNA hybridization, for detecting the strength of DNA chain interactions.

MATERIALS AND METHODS

Bovine serum albumin (BSA), lithium chloride, and polyoxyethylene-sorbitan monolaurate (Tween 20) are purchased from Sigma (St. Louis, MO). HEPES, EDTA solution (0.5M, pH8.0), and Tris-HCl buffers (pH 8.0) come from Fisher Scientific (Pittsburgh, PA). All oligonucleotides are custom-synthesized and purified with high-performance liquid chromatography by Biosource International (Camarillo, CA). Succinmidyl 4-[p-maleimidophenyl]butyrate (SMPB) and BupH modified Dulbecco's phosphate buffered saline (PBS) were purchased from Pierce Biotechnology (Rockford, IL). Superavidin-coated polystyrene microspheres of 5.5 μm diameter are products of Bangs Laboratories (Fishers, IN).

Substrate preparation

For the preparation of substrates, we adapted methods described in literature (36). Briefly, ordinary 25 mm $\times$ 75 mm microscope slides pretreated with piranha solution (2:1 concentrated H_2SO_4:30% H_2O_2) are immersed in the silanization solution (2% solution of 3-aminopropyltriethoxysilane in 95:5 MeOH:1 mM aqueous acetic acid) for 40 min, followed by washing with methanol and drying in the oven. Cured slides are treated with SMPB, thiolated single-stranded oligonucleotides, and 50 mM sodium phosphate, 1 M NaCl, pH 6.5 buffer in order. After rinsing with water, the slides are spin dried and ready for hybridization.

Thiolated single-stranded oligonucleotide sequences are protected in water containing 0.01 M dithiothreitol when delivered. A G-25 spin column (Amersham Biosciences, Piscataway, NJ) is used to remove dithiothreitol from the sample, followed by solubilization in HEPES (10 mM HEPES, 5 mM EDTA, pH 6.6) to dilute the sample to a concentration of 25 μM. This diluted sample is used to coat the slide to link the molecules to the slide surface covalently.

To characterize the DNA coverage on the slide surface, we coat the surface with thiolated oligonucleotides tagged with Cy5 dye. The slides are then scanned with ScanArray 5000 (PerkinElmer Life and Analytical Sciences, Wellesley, MA) and the fluorescent intensity is compared with that of a calibration slide (Full Moon Biosystems, Sunnyvale, CA). The calibration curve from this commercial slide (fluorescent intensity versus number of fluorochromes per unit area) is used to find DNA densities on our slide surfaces.

Microsphere preparation

Biotinylated single-stranded oligonucleotides are linked to the bead surface via avidin-biotin bonds, using the method recommended by the manufacturer, as follows (37): The beads are rinsed with TTL buffer (100 mM Tris-HCl, pH 8.0; 0.1% Tween 20; and 1 M LiCl) twice, then incubated in biotinylated oligonucleotide solution and TTL buffer mixture for 1 h. The oligonucleotide-microsphere conjugates are washed with 0.15 N NaOH, rinsed with TT buffer (250 mM Tris-HCl, pH 8.0, 0.1% Tween 20) twice, and incubated in TTE buffer (250 mM Tris-HCl, 0.1% Tween 20, 20 mM Na_2EDTA, pH 8.0) at 80°C for 10 min. The conjugates are suspended in solution of 2% denatured BSA in PBS at 4°C overnight before use.

To characterize the DNA coverage on bead surface, we use flow cytometry to measure the fluorescent intensities on bead surfaces and convert them into DNA densities, using the calibration curve relating the mean peak fluorescence of Quantum 26 calibration beads to their molecules of equivalent soluble fluorochrome (23).

Flow adhesion assay

Adhesion experiments are performed in a custom-manufactured parallel-plate flow chamber, whose bottom surface is the glass slide coated with single-stranded oligonucleotides. The whole assembly is mounted on the stage of a Nikon Diaphot inverted microscope with phase-contrast optics (Nikon, Tokyo, Japan). A gasket with a tapered cutout prepared from 0.01-inch-thick Duralastic sheeting (Allied Biomedical, Goose Creek, SC) is used to regulate the flow with different shear rate in each axial position along the same slide. Flow is initiated with a syringe pump. Microspheres suspended in the running buffer are connected to the inlet of the flow chamber by a rubber tube and brought into the chamber by a gentle flow. The microspheres are allowed to settle on the slide surface without flow until adhesion steady state is reached (required incubation time varies with the type of DNA molecule used, data not shown), and then the microspheres are detached from the slide surface with controlled flow. Pictures at randomly selected points on the slide before and after the controlled flow started are recorded with a Cohu black and white charge-coupled device camera (Cohu, San Diego, CA) and Sony SVO-9500MD S-VHS recorder (Sony Medical Systems, Montvale, NJ). The locations of these points are shown with a digital dimension indicator attached to the microscope stage, from which the corresponding shear rates are derived according to

$$\gamma = \frac{6Q}{h^2 w_1}\left(1 - \frac{z}{L}\right), \tag{1}$$

where w_1 is the width at the channel entrance in centimeters, z is the axial position from the inlet, and L is the channel length. Q is the volumetric flow rate. h is the channel height, which is measured by focusing the microscope on the top and bottom surfaces (23).

The recorded pictures are analyzed and the bead numbers are counted through digital image analysis with LabVIEW software (National Instruments, Austin, TX). Microsphere adhesion is quantified by the ratio of the numbers of beads in the same visual field under the microscope at a given position on slides after and before the flow is applied. Typically, the bead number varies between 80 and 130 in a single field of view before the detachment flow starts. As the data analysis considers the behavior of the whole bead population instead of a single bead, the difference among individual beads caused by the randomness of the DNA coverage is averaged out. Moreover, all the data shown in this article are average results of at least six independent experiments to minimize the variation among different slide surfaces. Error bars are plotted using standard error calculations.

Fluorescent DNA hybridization assay

Thiolated ssDNA molecules (types 30**b**, 30**b**(7), 30**b**(10), and 30**b**(15) (see below)) are spotted on the SMPB modified glass slide with pipette and immobilized as described above. The hybridization buffer is 2% denatured BSA in PBS (pH 7.4). These immobilized DNA samples are incubated for 30 min at room temperature with 0.2 μM Cy5-30**a** in hybridization buffers. The slide is then washed with the same buffer containing 0.1% sodium dodecyl sulfate at room temperature for 15 min, followed by rinsing in DI water. The spin dried slide is scanned with ScanArray 5000 (PerkinElmer) and the fluorescent intensity is quantified with ScanArray Express software.

RESULTS

Design of oligonucleotide sequences

We designed two pairs of complementary oligonucleotide sequence molecules consisting of 30 bases in each molecule. One pair was 30**a** and 30**b**; the other pair was 30**c** and 30**d**. Strands 30**a** and 30**b** are complementary to each other, and 30**c** is complementary to 30**d**. Other sequences used in this

article are derived from these molecules. Shorter molecules are obtained by removing some bases from the sequence 30**a** and 30**b**, and mismatched molecules are obtained by mutating a single base in the sequence of 30**b** or 30**d** (Tables 1 and 2). Within each molecule, 10 bases at 5′ end are used as spacers from the bead and substrate surfaces to ensure better hybridization efficiency (38–40). Self-melting temperatures of individual strands are much lower than the ambient temperature (20–21°C) to avoid hairpin folding of sequences (38–40). Duplex melting temperatures are between 50°C and 90°C, in accordance with the guidance of design of primers in biology experiments. All DNA molecules denoted with an ''**a**'' or ''**c**'' are immobilized on beads, whereas the complementary sequences denoted with a ''**b**'' or ''**d**'' are immobilized on slides. Fig. 1 illustrates the design of the experiments.

DNA coverage on slide and microsphere surfaces

As indicated in the methods, we measured the density of DNA strands on the substrate. On slide surfaces, DNA site density decreases with the increasing length of immobilized molecules for the same solution concentration of molecule during the incubation (Fig. 2). Likewise, larger lengths of chains on bead surfaces (exceeding 22 bases in length) led to a decrease in surface coverage on the bead. Sequences shorter than 22 bases resulted in negligible differences in DNA density for the same solution concentration of oligonucleotide chain.

Specific adhesion of microspheres mediated by DNA hybridization

To test the specificity of the adhesion of nucleotide-coated microspheres, single-stranded oligonucleotide 30**a**-coated microspheres are incubated with the slide surfaces functionalized with patches of 30**a** and 30**b**, and then a gentle flow at a shear rate of $\sim 500\ s^{-1}$ is used to remove unbound or weakly bound beads. Beads remaining on the slide after the flow are assumed to remain because of hybridization between complementary sequences on bead and slide surfaces. Our results (Fig. 3) show that the DNA-functionalized microspheres bind firmly only to regions functionalized with complementary DNA sequences; that is, 30**a**-coated microspheres only bind to patches coated with complementary 30**b,** whereas almost no 30**a**-coated microspheres bind to the noncomplementary DNA coated surfaces or those regions devoid of DNA.

Effects of shear rate and salt concentration in microsphere detachment

Salt concentration can alter the affinity of DNA hybridization. To illustrate the effect of salt concentration on microsphere adhesion, the strength of adhesion between microspheres coated with 24**a** molecules and slide surfaces coated with the complementary 24**b** molecules was measured. Running buffer, which also serves as the hybridization buffer, is 2% denatured BSA in PBS containing different concentrations of sodium chloride, as indicated in Fig. 4. Bead adhesion is plotted as a function of shear rate at different concentrations of NaCl. For all salt concentrations, beads bind to the slide tightly at low shear rates. With increasing shear rate, more and more beads are detached from the slide surface. At the highest shear rates, almost all of the beads are removed. To compare the relative adhesive strength of DNA duplexes as a function of overlap length, sequence defects, and salt concentration, we define a critical shear rate (γ_c) as the shear rate necessary to remove 50% of the adherent beads. As shown in Fig. 4, we find that increasing ionic strength leads to increasing critical shear rate. This is expected and in accord with the known effect that salt suppresses repulsion between hybridizing DNA strands, and the interchain melting temperature increases with increasing salt concentration (41).

TABLE 1 Perfectly complementary DNA pairs with different length of segment overlap

Name	Sequence	Self melting temperature (40) (°C)	Melting temperature (39,44) (°C)
30**b**	5′-TTTTTTTTTT**TGCCTTGTCTAATATCCGTA**-3′	−17.6	81.0
30**a**	5′-TTTTTTTTTT**TACGGATATTAGACAAGGCA**-3′	7.6	
28**b**	5′-TTTTTTTTTT**CCTTGTCTAATATCCGTA**-3′	−9.3	76.5
28**a**	5′-TTTTTTTTTT**TACGGATATTAGACAAGG**-3′	7.6	
26**b**	5′-TTTTTTTTTT**TTGTCTAATATCCGTA**-3′	−7.3	73.0
26**a**	5′-TTTTTTTTTT**TACGGATATTAGACAA**-3′	−1.8	
24**b**	5′-TTTTTTTTTT**GTCTAATATCCGTA**-3′	−7.3	69.9
24**a**	5′-TTTTTTTTTT**TACGGATATTAGAC**-3′	−15.8	
22**b**	5′-TTTTTTTTTT**CTAATATCCGTA**-3′	−7.3	65.3
22**a**	5′-TTTTTTTTTT**TACGGATATTAG**-3′	−15.8	
18**b**	5′-TTTTTTTTTT**TATCCGTA**-3′	−17.6	58.5
18**a**	5′-TTTTTTTTTT**TACGGATA**-3′	−22.4	
30**d**	5′-TTTTTTTTTT**TAGGAAGGTGATAATGGTGT**-3′	−16.7	81.4
30**c**	5′-TTTTTTTTTT**ACACCATTATCACCTTCCTA**-3′	−44.0	

Ten thymine bases are used as the spacer in each molecule, and the actual hybridizing segment is represented in bold letters. The melting temperatures calculations are based on the lower DNA concentrations on bead surfaces (compared to substrate surfaces). Salt concentration is taken as 1 M sodium chloride, according to the experimental conditions.

TABLE 2 DNA sequences with one base mismatched when hybridize with 30a or 30c molecule

Name	Sequence	Self melting temperature (°C) (40)	Melting temperature (39,47)(°C)
30**b**(7)	5′-TTTTTTTTTT**TGCCTTGTCTAAT*T*TCCGTA**-3′	2.3	77.1
30**b**(10)	5′-TTTTTTTTTT**TGCCTTGTCT*T*ATATCCGTA**-3′	−17.6	77.1
30**b**(15)	5′-TTTTTTTTTT**TGCCT*A*GTCTAATATCCGTA**-3′	−17.6	77.7
30**d**(7)	5′-TTTTTTTTTT**TAGGAAGGTGATA*T*TGGTGT**-3′	−2.1	75.5
30**d**(10)	5′-TTTTTTTTTT**TAGGAAGGTG*T*TAATGGTGT**-3′	5.4	75.6
30**d**(15)	5′-TTTTTTTTTT**TAGGA*T*GGTGATAATGGTGT**-3′	−2.2	76.1

The mutation point is represented with underlined italic letters. The numbers in parenthesis in sequence names represent the mutation sites counting from the 3′ end. Melting temperatures are the ones when they hybridize with 30**a** (for 30**b** derivatives) or 30**c** (for 30**d** derivatives) molecules.

Effects of degree of chain overlap on bead detachment

The effect of the number of basepair matches on the adhesive strength of DNA-coated microspheres is illustrated in Fig. 5. In general, the detachment curves all have similar shape, but the curves shift rightward to higher shear stresses with increasing chain overlap. As illustrated in Fig. 5 *B*, in this range of overlap lengths, the critical shear rate is linear with the segment overlap length in this assay. This confirms that the adhesion strength for these relatively short DNA duplexes can be correlated with overlap length of hybridized DNA chains, and that the adhesion strength can be used as a metric of the length of chain overlap.

Effects of point mutation in hybridization on bead detachment

The effect of point mutations on DNA-mediated adhesive strength is illustrated in Fig. 6. Bead detachment is shown in Fig. 6 *A* for perfectly complementary 20 basepair overlap lengths (30**a**:30**b**) and for otherwise equivalent sequences with a point mutation located at the seventh base in the **b** strand (30**a**:30**b**(7)). As expected, the presence of the mutation decreases the critical shear rate (adhesion strength) compared to that of perfectly matched 30**a**:30**b** sequences. Interestingly, it is shown that the adhesion strength for 30**b**(7) pairs is close to that of two perfectly complementary DNA chains of 15 base overlap (Fig. 6 *B*). This result indicates that the correctly matched 13 bases at the 5′ end of 30**b**(7) is not the only contribution to hybridization, and that six bases at the 3′ end supplements the DNA-DNA binding.

Then, we altered the location of the mutated base. A point mutation was introduced at either the 10th (30**b**(10)) or the 15th (30**b**(15)) base in the hybridization segment, respectively. Our results shown in Fig. 6 *C* indicate the critical

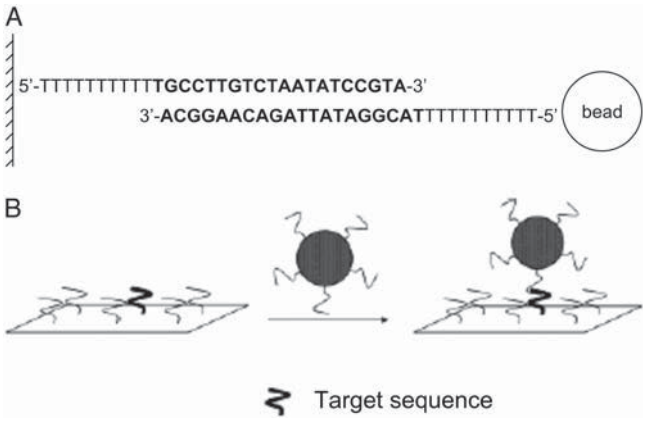

FIGURE 1 (*A*) Complementary DNA sequence 30**a** is immobilized on bead surface while 30**b** is immobilized on the slide surface. The first 10 bases of thymine on each sequence next to the bead and substrate surfaces function as spacers, and the overlapping hybridization segments parts are represented in bold letters. (*B*) Schematic diagram of microspheres binding to the slide surface mediated by DNA hybridization.

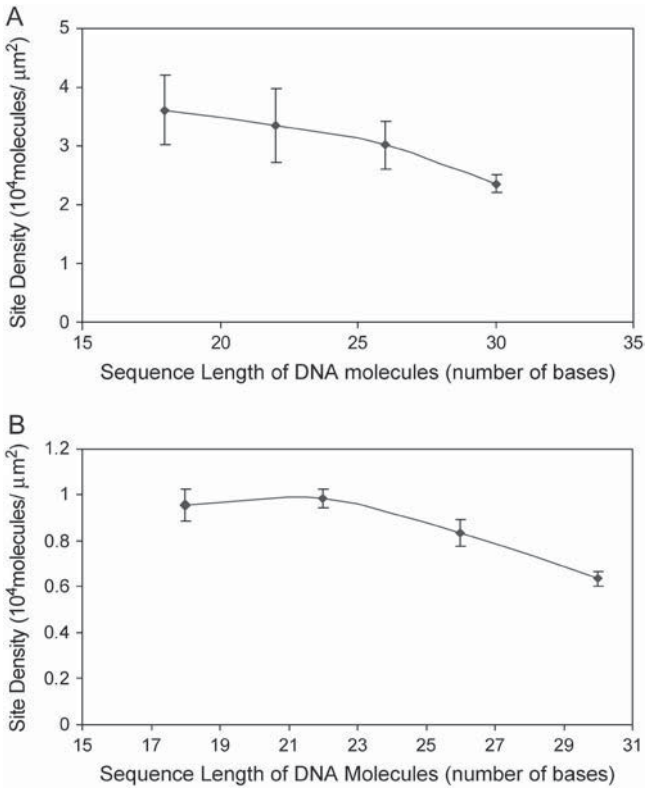

FIGURE 2 DNA site density as a function of sequence length on (*A*) glass slide and (*B*) bead.

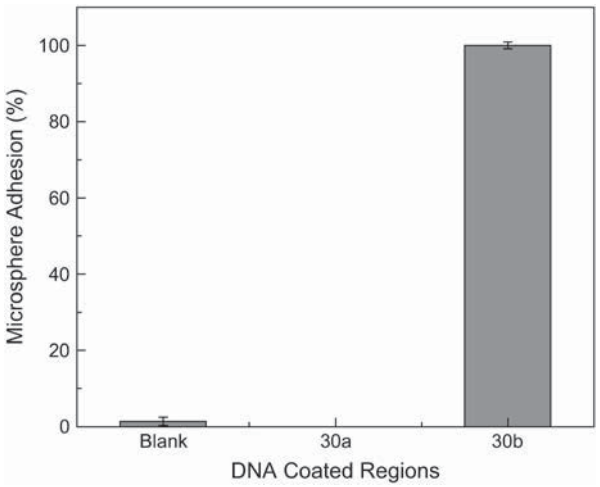

FIGURE 3 Specific adhesion of microspheres to a glass slide mediated by DNA hybridization. The microspheres are coated with 30**a** molecules, and slide surfaces are coated with 30**a** (noncomplementary) and 30**b** (complementary).

shear rates for single-nucleotide polymorphisms (SNP)-containing sequences is smaller than that of fully complementary molecules if the defect is at the 15th base, but not if the defect is at the 10th base. Since we showed previously that a SNP is detectable if the defect is at the seventh base, this suggests the some defects are detectable using this method, depending on the location of the defect.

To determine if these results were an effect of sequence chemistry, we measured the adhesion strengths mediated by a different pair of perfectly complementary DNA (30**c** and 30**d**) strands, as well as with strands with SNPs. Single base mismatches were introduced at the same positions—seventh, 10th, and 15th base—of 30**d**. Results in Fig. 6 *D* show a

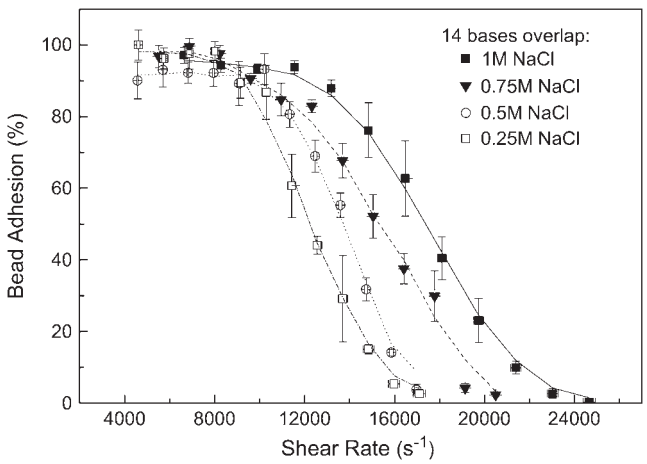

FIGURE 4 Effects of wall shear rate on bead adhesion mediated by DNA hybridization in PBS hybridization buffers of varying ionic strength. The beads are coated with 24**a** molecules, and slides are functionalized with 24**b** sequences. There are 14 bases that overlap between the DNA pairs.

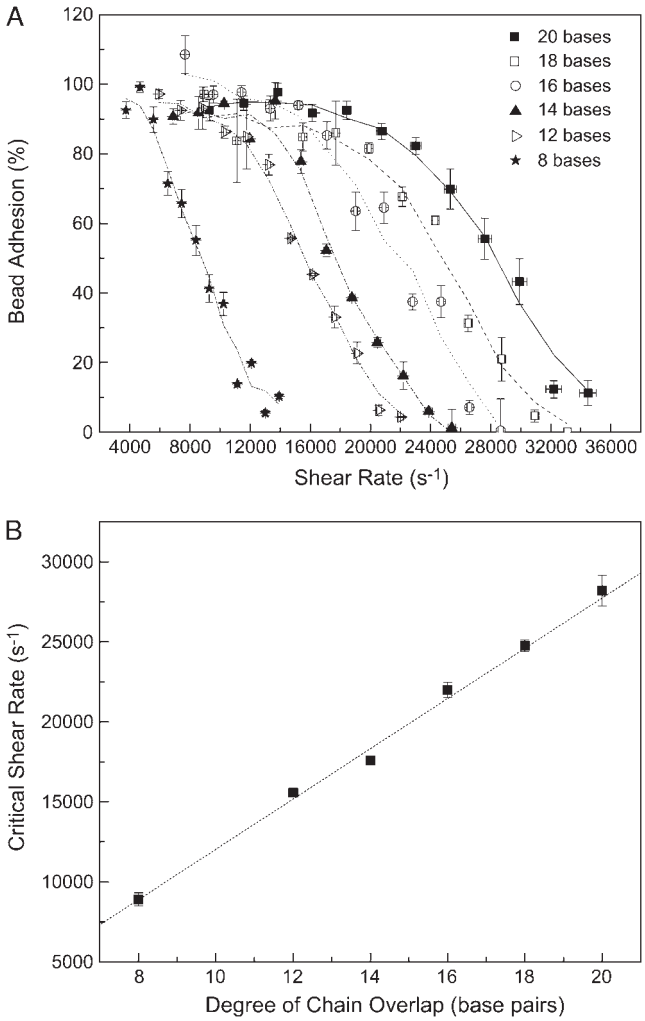

FIGURE 5 Bead adhesion mediated by molecules from **a**:**b** series. (*A*) Effects of wall shear rates on bead adhesion mediated by DNA pairs with different length of chain overlap. (*B*) Effects of degree of chain overlap on critical shear rate. The critical shear rates are obtained from the curves in part *A*, where ''critical'' refers to the shear rate that leads to a decrease in adhesion of 50%.

significant difference in critical shear rates for all of these locations of SNP-containing molecules, and confirm the bead adhesion assay can selectively determine SNPs. Furthermore, with 30**c**-30**d** strands, the force of adhesion is independent of the location of the defect. These results show that although SNPs can be detected, the effect of the SNP location depends on chain chemistry.

DISCUSSION

In this article, we investigate microsphere adhesion mediated by hybridization of oligonucleotide sequences. The microsphere adhesion is highly specific. Quantitative measurements show a majority of beads are adherent to the positive sample regions, whereas almost no nonspecific binding to

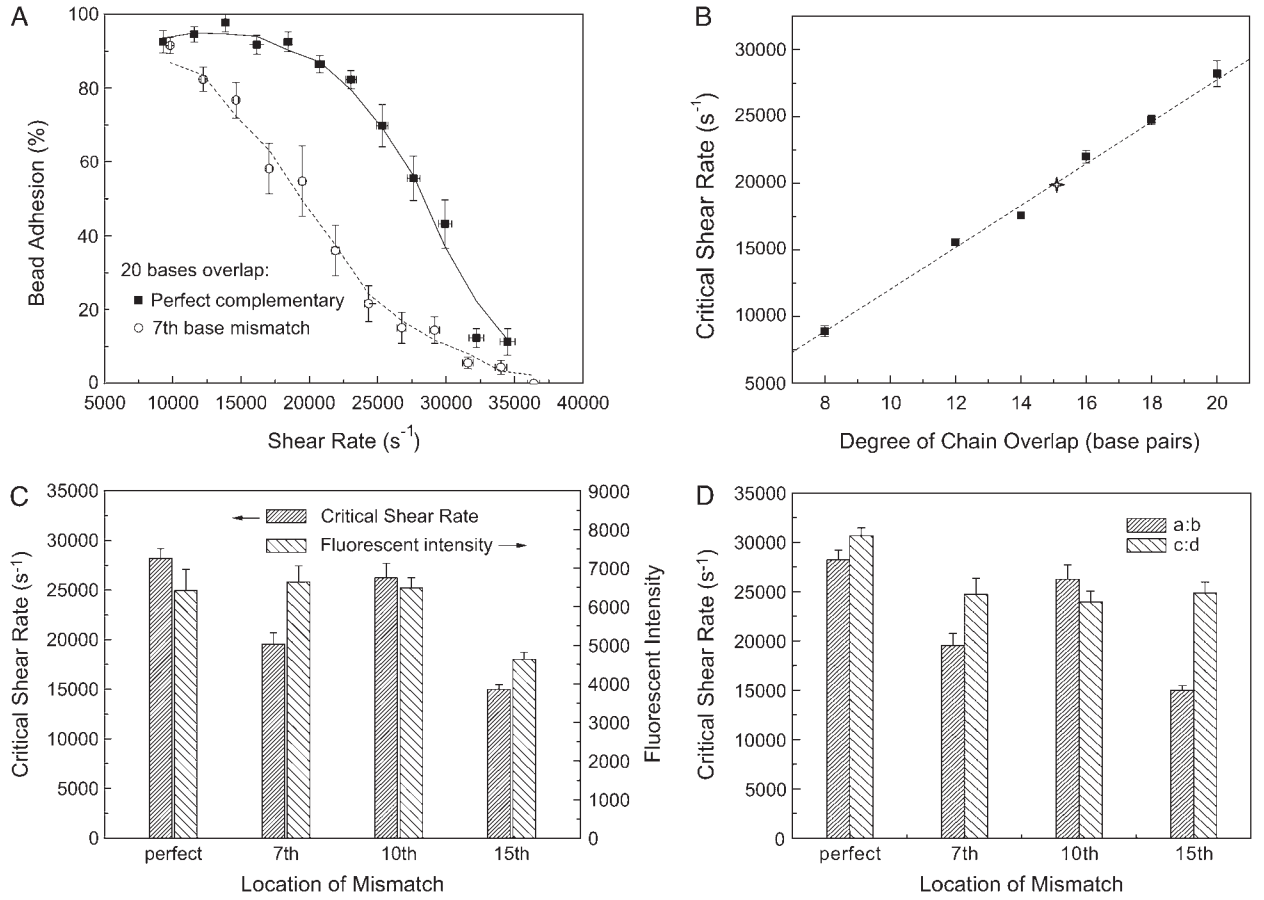

FIGURE 6 Effects of point mutation on bead adhesion strength. (*A*) Comparison of bead adhesion mediated by perfect hybridization (30**a**:30**b**) and hybridization with the seventh base mismatched (30**a**:30**b**(7)). (*B*) Comparison of critical shear rates for adhesion mediated by hybridization with the seventh base mismatched (labeled with the *star*) and perfectly matched hybridizations with different degrees of chain overlap (**a**:**b** series). (*C*) Comparison of selectivity between bead adhesion assay and fluorescent hybridization assay (**a**:**b** series), which determines the density of matching chains. (*D*) Effects of location of point mutation on critical shear rate. All the DNA pairs have 20 bases overlap, within which one base was mismatched. The mutation sites are counted from the 3′ end of the molecules immobilized on slide surfaces.

negative regions (Fig. 3). Hydrodynamic force is used to select between well-bound and weakly bound beads. We are exploiting an effect that the strength of DNA-DNA duplex binding is a function of the length of chain overlap (1,4). Higher shear rates produce stronger external forces on each bead, which in turn are imparted on the DNA duplexes. When the force is large enough, the weakest linkage connecting beads to the slide—in our case, DNA-DNA association—is broken and the beads are detached from the slide and removed from the flow chamber. Fig. 4 shows that the percentage of beads remaining adherent varies as a strong function of shear rate. For each specific buffer and specific type of DNA molecules, the ratio of bound beads to all initially bound beads decreases sharply within a specific shear rate range. This range is narrow enough to make us believe that most of the beads are bound to the slide with similar strength, and the critical shear rate is a sensitive parameter to reflect the chemistry of the hybridization. An explanation for the similarity in strength may be that during detachment, forces are focused on a very small number of identical bonds, and despite variations in the total number of adhesion molecules on beads throughout the population, detachment is an effect on a relatively small number of molecules (13). The critical shear rate increases with increasing salt concentration, reflecting the well-known fact that melting temperature increases with increasing salt concentration, since cations in salt neutralize the negative charges carried by DNA backbone and weaken the repulsion between the DNA chains, therefore increasing stability of the DNA double helix formed between beads and slide (41).

Dissociation of a DNA duplex requires a breakage of hydrogen bonds between two chains, as well as an overcome of the stacked base forces (7). Degrees of both forces depend highly on the length of chains. In our study, beads are shown to adhere to the slide surface with higher strength when their adhesion is mediated by longer DNA molecules (Fig. 5). Remarkably, the adhesion strength determined by this bead assay increases linearly with the degree of chain overlap.

Although there are slight differences in chain density as a function of chain length (owing to differences in adsorption on the slide and bead surfaces (Fig. 2)), we conclude that the length of the hybridized portion of the DNA molecules, not the chain density, plays the dominant role in controlling adhesion strength. It may be possible for us ultimately, with the use of mechanochemical models (42), to deduce the strength of single DNA duplexes from proper analysis of these detachment experiments.

The equilibrium dissociation constant, K_D, is defined as the ratio of forward and reverse reaction rates, and determines how many ssDNA form duplex at steady state of the hybridization reaction (43). In regular DNA microarray experiments, K_D is the only selective factor, since fluorescent intensity depends solely on the amount of labeled molecules remaining bound after washing. However, in our bead-adhesion system, the dissociation force of individual DNA duplex also plays an important role in adhesion strength: the adhesion strength becomes larger if the individual bond is stronger (11). Starting with a system where there are 20 overlapping bases when the system is perfectly matched (30**a**:30**b**), we explored the effect of strategically placed single-base mismatches at the seventh, 10th, and 15th location on bead adhesion, and compared the results with those from a regular fluorescent hybridization assay. As shown in Fig. 6 *C*, regular microarray assay showed the same level of fluorescent intensities for the perfectly complementary pairs and those containing a mismatch (30**a**:30**b**(7), 30**a**:30**b**(10)), whereas the bead adhesion strength decreased 31% and 7%, respectively. This result suggests the location of the defect affects the strength of adhesion. Given that the thermodynamics (K_D) of binding between 30**a**:30**b**(15) is very similar to that of the other two defective pairs (30**a**:30**b**(7), 30**a**:30**b**(10)) (44), the much weaker fluorescence for 30**a**:30**b**(15) suggests the possibility of lower DNA coverage (36). Therefore, it is reasonable for us to normalize adhesion strength sample based on the density of chains. If we do so, we derive that the adhesion strength decreases 26% because of the single base mismatch on 15th base in **b** strand. Therefore, defects at the seventh and 15th position lead to significant decreases in adhesion strength, and an SNP is detectable using this assay.

Interestingly, a defect at the seventh position shows the adhesiveness of a perfectly matched 15 basepair sequence, indicating some contributions from the segment on the 3′ side of the defect in the **b** strand. We tested whether this result was sequence dependent using another pair of perfectly complementary molecules (30**c**:30**d**) and their defective derivatives (30**c**:30**d**(7), 30**c**:30**d**(10), 30**c**:30**d**(15)). Results shown in Fig. 6 *D* indicate that for all the derivatives in **c**:**d** series, the bead adhesion strengths decrease ~20% from that of perfectly complementary pairs (30**c**:30**d**). Furthermore, based on the fact that these chains display similar fluorescent intensities (therefore similar coverage density of DNA duplex), we conclude that the difference in adhesion strength results from the different dissociation force depending on the location of the defect in the DNA duplex. Molecules containing single base mismatch are less stable than perfectly complementary ones, and weaker force is required to separate the two strands. This conclusion is in agreement with results from single molecule experiments (7). These results indicate that the effect of mismatch location on bead adhesion strength/dissociation force is sequence-dependent, which explains why conclusions from literature regarding this point are inconsistent (7,45). The results from 30**a**:30**b** sequences, however, suggest that adhesion strength is not solely determined by the thermodynamics of association (since different locations of defects give the same K_D yet different adhesion strengths).

K_D is predicted to have a very small value for most DNA pairs in this article, based on computational algorithms or reports from the literature (44), so it is reasonable to assume that most of the molecules in the contact region will form bonds (13). Further, we clarify that flow is only used after the beads are fully bound. Therefore, even though buffer flow may change the configuration and orientation of DNA molecules in the system (46), this is expected to have a minor effect on the results. By far the predominant result is the effect of hydrodynamics on chain dissociation.

CONCLUSION

In this study, we develop a novel method to study the physics of DNA binding in adhesive interface with hydrodynamic flow, using adhesion of micron-sized beads. It is proved that the beads bind to complementary samples on slide surface with specificity. The adhesion strength can be correlated to the salt concentration in hybridization buffer, degree of chain overlap, and the defective basepair in hybridization. Therefore, these experiments represent a specific and reproducible means for studying the hybridization of multiple DNA chains, and also hold the potential to detect the chemistry of unknown DNA molecules. Forthcoming analysis using adhesion dynamics simulation (13) will allow us to estimate the bond number between each bead and slide surface, and therefore deduce molecular binding properties from comparison to experiments.

We gratefully acknowledge financial support from the National Science Foundation Bioengineering and Environmental Systems 03-14265.

REFERENCES

1. Lee, G. U., L. A. Chrisey, and R. J. Colton. 1994. Direct measurement of the forces between complementary strands of DNA. *Science*. 266: 771–773.
2. Noy, A., D. V. Vezenov, J. F. Kayyem, T. J. Meade, and C. M. Lieber. 1997. Stretching and breaking duplex DNA by chemical force microscopy. *Chem. Biol.* 4:519–527.
3. Pope, L. H., M. C. Davies, C. A. Laughton, C. J. Roberts, S. J. Tendler, and P. M. Williams. 2001. Force-induced melting of a short DNA double helix. *Eur. Biophys. J.* 30:53–62.

4. Strunz, T., K. Oroszlan, R. Schafer, and H. J. Guntherodt. 1999. Dynamic force spectroscopy of single DNA molecules. *Proc. Natl. Acad. Sci. USA.* 96:11277–11282.
5. Bell, G. I. 1974. Model for the binding of multivalent antigen to cells. *Nature.* 248:430–431.
6. Chang, K. C., and D. A. Hammer. 2000. Adhesive dynamics simulations of sialyl-Lewis(x)/E-selectin-mediated rolling in a cell-free system. *Biophys. J.* 79:1891–1902.
7. Sattin, B. D., A. E. Pelling, and M. C. Goh. 2004. DNA base pair resolution by single molecule force spectroscopy. *Nucleic Acids Res.* 32:4876–4883.
8. Jin, R., G. Wu, Z. Li, C. A. Mirkin, and G. C. Schatz. 2003. What controls the melting properties of DNA-linked gold nanoparticle assemblies? *J. Am. Chem. Soc.* 125:1643–1654.
9. Taton, T. A., C. A. Mirkin, and R. L. Letsinger. 2000. Scanometric DNA array detection with nanoparticle probes. *Science.* 289:1757–1760.
10. Park, S. J., T. A. Taton, and C. A. Mirkin. 2002. Array-based electrical detection of DNA with nanoparticle probes. *Science.* 295:1503–1506.
11. Swift, D. G., R. G. Posner, and D. A. Hammer. 1998. Kinetics of adhesion of IgE-sensitized rat basophilic leukemia cells to surface-immobilized antigen in Couette flow. *Biophys. J.* 75:2597–2611.
12. Kuo, S. C., and D. A. Lauffenburger. 1993. Relationship between receptor/ligand binding affinity and adhesion strength. *Biophys. J.* 65: 2191–2200.
13. Kuo, S. C., D. A. Hammer, and D. A. Lauffenburger. 1997. Simulation of detachment of specifically bound particles from surfaces by shear flow. *Biophys. J.* 73:517–531.
14. Eniola, A. O., S. D. Rodgers, and D. A. Hammer. 2002. Characterization of biodegradable drug delivery vehicles with the adhesive properties of leukocytes. *Biomaterials.* 23:2167–2177.
15. Bhatia, K. S., and D. A. Hammer. 2002. Influence of receptor and ligand density on the shear threshold effect for carbohydrate-coated particles on L-selection. *Langmuir.* 18:5881–5885.
16. Brunk, D. K., and D. A. Hammer. 1997. Quantifying rolling adhesion with a cell-free assay: E-selectin and its carbohydrate ligands. *Biophys. J.* 72:2820–2833.
17. Rodgers, S. D., R. T. Camphausen, and D. A. Hammer. 2001. Tyrosine sulfation enhances but is not required for PSGL-1 rolling adhesion on P-selectin. *Biophys. J.* 81:2001–2009.
18. Knudsen, S. 2002. A Biologist's Guide to Analysis of DNA Microarray Data. John Wiley & Sons, New York.
19. Reichert, J., A. Csaki, J. M. Kohler, and W. Fritzsche. 2000. Chip-based optical detection of DNA hybridization by means of nanobead labeling. *Anal. Chem.* 72:6025–6029.
20. Southern, E. M. 1996. DNA chips: analysing sequence by hybridization to oligonucleotides on a large scale. *Trends Genet.* 12:110–115.
21. Southern, E. M. 2001. DNA microarrays. History and overview. *Methods Mol. Biol.* 170:1–15.
22. Heller, M. J. 2002. DNA microarray technology: devices, systems, and applications. *Annu. Rev. Biomed. Eng.* 4:129–153.
23. Zhang, Y., A. O. Eniola, D. J. Graves, and D. A. Hammer. 2003. Specific adhesion of micron-sized colloids to surfaces mediated by hybridizing DNA chains. *Langmuir.* 19:6509–6511.
24. Bao, P., A. G. Frutos, C. Greef, J. Lahiri, U. Muller, T. C. Peterson, L. Warden, and X. Xie. 2002. High-sensitivity detection of DNA hybridization on microarrays using resonance light scattering. *Anal. Chem.* 74:1792–1797.
25. Csaki, A., R. Moller, W. Straube, J. M. Kohler, and W. Fritzsche. 2001. DNA monolayer on gold substrates characterized by nanoparticle labeling and scanning force microscopy. *Nucleic Acids Res.* 29:E81.
26. Taton, T. A., G. Lu, and C. A. Mirkin. 2001. Two-color labeling of oligonucleotide arrays via size-selective scattering of nanoparticle probes. *J. Am. Chem. Soc.* 123:5164–5165.
27. Cao, Y. C., R. Jin, and C. A. Mirkin. 2002. Nanoparticles with Raman spectroscopic fingerprints for DNA and RNA detection. *Science.* 297:1536–1540.
28. Miller, M. M., P. E. Sheehan, R. L. Edelstein, C. R. Tamanaha, L. Zhong, S. Bounnak, L. J. Whitman, and R. J. Colton. 2001. A DNA array sensor utilizing magnetic microbeads and magnetoelectronic detection. *J. Magn. Magn. Mater.* 225:138–144.
29. Schatz, G. C., M. Schuster, K. Berlin, and A.-G. Epigenomics. Germany, assignee. 2004. Detecting nucleic acid sequences with probes containing a mass-labeled moiety connected to the probe by a labile bond. Germany patent DE 10240746.
30. Furtado, L. M., and M. Thompson. 1998. Hybridization of complementary strand and single-base mutated oligonucleotides detected with an on-line acoustic wave sensor. *Analyst.* 123:1937–1945.
31. Cho, Y. K., S. Kim, G. Lim, and S. Granick. 2001. A surface forces study of DNA hybridization. *Langmuir.* 17:7732–7734.
32. Jensen, K. K., H. Orum, P. E. Nielsen, and B. Norden. 1997. Kinetics for hybridization of peptide nucleic acids (PNA) with DNA and RNA studied with the BIAcore technique. *Biochemistry.* 36: 5072–5077.
33. Persson, B., K. Stenhag, P. Nilsson, A. Larsson, M. Uhlen, and P. Nygren. 1997. Analysis of oligonucleotide probe affinities using surface plasmon resonance: a means for mutational scanning. *Anal. Biochem.* 246:34–44.
34. Tawa, K., and W. Knoll. 2004. Mismatching base-pair dependence of the kinetics of DNA-DNA hybridization studied by surface plasmon fluorescence spectroscopy. *Nucleic Acids Res.* 32:2372–2377.
35. Chang, K. C., and D. A. Hammer. 1999. The forward rate of binding of surface-tethered reactants: effect of relative motion between two surfaces. *Biophys. J.* 76:1280–1292.
36. Chrisey, L. A., G. U. Lee, and C. E. O'Ferrall. 1996. Covalent attachment of synthetic DNA to self-assembled monolayer films. *Nucleic Acids Res.* 24:3031–3039.
37. Bangs Laboratories. 1999. Instructions: ProActive Streptavidin Coated Microspheres. Fishers, IN.
38. Breslauer, K. J., R. Frank, H. Blocker, and L. A. Marky. 1986. Predicting DNA duplex stability from the base sequence. *Proc. Natl. Acad. Sci. USA.* 83:3746–3750.
39. Milam, V. T., A. L. Hiddessen, J. C. Crocker, D. J. Graves, and D. A. Hammer. 2003. DNA-driven assembly of bidisperse, micron-sized colloids. *Langmuir.* 19:10317–10323.
40. Zuker, M. 2003. Mfold web server for nucleic acid folding and hybridization prediction. *Nucleic Acids Res.* 31:3406–3415.
41. Kotin, L. 1963. On the effect of ionic strength on the melting temperature of DNA. *J. Mol. Biol.* 16:309–311.
42. Chang, K. C., and D. A. Hammer. 1996. Influence of direction and type of applied force on the detachment of macromolecularly-bound particles from surfaces. *Langmuir.* 12:2271–2282.
43. Krasik, E. F., and D. A. Hammer. 2004. A semianalytic model of leukocyte rolling. *Biophys. J.* 87:2919–2930.
44. SantaLucia, J., Jr., H. T. Allawi, and P. A. Seneviratne. 1996. Improved nearest-neighbor parameters for predicting DNA duplex stability. *Biochemistry.* 35:3555–3562.
45. Lee, I., A. A. Dombkowski, and B. D. Athey. 2004. Guidelines for incorporating non-perfectly matched oligonucleotides into target-specific hybridization probes for a DNA microarray. *Nucleic Acids Res.* 32:681–690.
46. Perkins, T. T., S. R. Quake, D. E. Smith, and S. Chu. 1994. Relaxation of a single DNA molecule observed by optical microscopy. *Science.* 264:822–826.
47. Peyret, N., P. A. Seneviratne, H. T. Allawi, and J. SantaLucia Jr. 1999. Nearest-neighbor thermodynamics and NMR of DNA sequences with internal A.A, C.C, G.G, and T.T mismatches. *Biochemistry.* 38:3468–3477.